# Testing and implementation of a transportable and robust radio-element mapping system

**AUTHOR:**
Jacques Bezuidenhout[1]

**AFFILIATION:**
[1]School for Science and Technology, Stellenbosch University, Faculty of Military Science, Stellenbosch, South Africa

**CORRESPONDENCE TO:**
Jacques Bezuidenhout

**EMAIL:**
jab@ma2.sun.ac.za

**POSTAL ADDRESS:**
Faculty of Military Science, Stellenbosch University, Private Bag X2, Saldanha 7395, South Africa

**DATES:**
**Received:** 08 Oct. 2014
**Revised:** 04 Dec. 2014
**Accepted:** 06 Feb. 2015

**KEYWORDS:**
gamma ray spectroscopy; scintillation detector; in-situ measurements; naturally occurring radionuclides; geographical information systems

**HOW TO CITE:**
Bezuidenhout J. Testing and implementation of a transportable and robust radio-element mapping system. S Afr J Sci. 2015;111(9/10), Art. #2014-0350, 7 pages. http://dx.doi.org/10.17159/sajs.2015/20140350



Gamma ray spectroscopy has been successfully applied as a survey tool in the fields of morphology, geology and mineral exploration. Gamma ray surveys are regularly done at ground level, which frequently requires transecting remote and unforgiving environments. Thus a need for the development of a transportable, robust and portable gamma ray detection system was identified. In addition to collecting radiation data, such a system was required to also provide the geographic position of the data and allow for various analyses tools to be utilised in the field. These functions were achieved by integrating a USB-driven scintillation detector with a field tablet and creating software to control acquisition and analyses of radiation data, as well as logging position. The system was tested in different geographical locations under different modes of transport. The instrument was tested by employing several different methods of data analysis in order to extract natural nuclide condensations. The consistency in the obtained data demonstrated the reliability of the instrument in the different environments. The system also successfully replicated previous radio-element survey findings and provided information on several geographical phenomena, including information on the geology, paved road structure and beach sediment characteristics.

## Introduction

Radio-element mapping is utilised in various fields of research at different locations across southern Africa. These research locations are frequently difficult to access and environmental conditions tend to be extreme. Such areas include stretches of remote coastlines, deserts and mountains. Access to the areas therefore poses a great challenge to researchers who employ radiation-measuring techniques. Mapping of radionuclide concentrations has in the past required the time-intensive practice of sediment sampling or stationary in-situ measurements, both of which limit the number of sampling points and usually require post processing.

Transportable in-situ gamma ray spectrometry measurement techniques have been developed by several organisations[1-3] in order to measure larger areas more effectively. This motivated the development of a unique, cost-effective and transportable measuring system suitable for the local geographical environment in southern Africa. Various means of transportation of gamma ray measuring systems are possible and include aircraft, motor vehicle and even on foot. However, the mode of transportation must be carefully selected, taking into consideration the research requirements and the geographical factors of the research area. Most of these modes of transportation subsequently require a robust and modular system that is capable of multiplatform deployment. The system needs to have an extended battery capability but also must be lightweight to ensure measurements can be conducted on foot. The system also requires a global positioning system (GPS) to record position while surveying in remote study areas.

The most significant naturally occurring radionuclides are uranium ($^{238}$U), thorium ($^{232}$Th) and potassium ($^{40}$K), of which potassium is by far the most abundant and fluctuating.[4] Distinctive concentrations of these naturally occurring radionuclides usually indicate important geophysical phenomena which must be thoroughly investigated while on location. On-site indication of such geographical phenomena helps to guide the system operator to ensure sufficient field data are recorded that can later be used for further processing and investigation. The system must therefore provide the operator with real-time information on changes in the naturally occurring radionuclides in order to allow for the operator to modify data collection accordingly.

In-situ gamma ray spectra can be analysed through various methods[1,5-7] in order to more accurately extract nuclide concentrations. The acquisition of these spectra is managed by software and some of this software provides access and control over the methods that are employed for data analysis. The ideal is that the researcher should have the option of choosing between the preferred methods of analysis, or even be able to employ novel methods. The measuring systems should preferably have the functionality to allow the researcher to choose a method while on location.

A transportable in-situ gamma ray measurement system was consequently developed, taking all of the above-mentioned requirements into account. The system was tested in various geographical environments and the results were compared to the known physical factors of the test locations.

## Methods

### *Measuring system*

The measuring system consisted of a NaI(Tl) scintillation detector (Rexon Components Inc., NAI 3.0 PX 3.0 / 3.0 IV, Beachwood, NJ, USA), a digital multichannel analyser (MCA), a rugged tablet PC with an on-board GPS and real-time analysis software that controlled the entire system (Figure 1). The NaI(Tl) detector (76.2 mm x 76.2 mm) was coupled to the MCA and sealed in a padded case to protect the instruments from mechanical shock and dust. The scintiSPEC® MCA (http://gs.flir.com/) that is produced by FLIR® (Solingen, Germany) has a USB connection that acts as the power source for operation and allows data transfer. The combination of NaI(Tl) detector and


**Figure 1:** Photographs of the portable gamma ray detection system. (a) The system consisted of a 76.2 mm x 76.2 mm NaI(Tl) scintillation detector, a scintiSPEC multichannel analyser and a Trimble Yuma rugged tablet with an inbuilt GPS. The system mounted (b) on a quad motorcycle and (c) in a motor vehicle.

scintiSPEC® MCA was used in a previous experiment and proved to be suitable for in-situ measurements under local conditions.[8] The Trimble® Yuma (Yuma 2, Sunnyvale, CA, USA), a rugged tablet PC (http://www.trimble.com/), was chosen because of its on-board GPS and extended battery life.

The system settings and spectrum acquisition were controlled by the winTMCA32® software (which has 1024 channels) that is also produced by FLIR®. The program code was developed in the winTMCA32 software to analyse the spectra and obtain geographical locations, as well as export these data in a format compatible with the geographic information system (GIS). The winTMCA32 code directly acquired the geographic coordinates from the on-board GPS via a virtual communications port. The code also extracted the time-corrected counts from the various energy windows and combined the radiation data with the positions data. The code finally stored all hardware settings, in-situ spectra and the extracted results in files. The result files for these trials were read into and interpreted by Quantum GIS software.

The modified detector system was tested on three modes of transport. The system was initially mounted on a quad motorcycle with the detector fitted to the front metal structure of the motorcycle, 200 mm from the ground. The Yuma rugged tablet PC was mounted on the front carrier to make it easily accessible to the operator (Figure 1). The system was also carried on foot with the detector held at a height of 200 mm above the ground. Thirdly, the system was fitted inside a motor vehicle (Figure 1) and driven for several hours over distances of more than 300 km. The tablet PC was always mounted or carried in such a way that the operator had a clear view of the screen, as the system continuously provides radiation, position and timing information.

### *Calibrations*

Energy calibrations were performed before and after each period of measurements. The calibrations were performed in the range 0.2–2.7 MeV by using anthropogenic nuclides and natural environmental spectra. The following nuclides and associated gamma ray emissions were used for the energy calibration: $^{214}$Pb (351.3 keV), $^{137}$Cs (661.7 keV), $^{60}$Co (1173.2, 1332.5 keV), $^{40}$K (1460.8 keV), $^{214}$Bi (1764.5 keV) and $^{208}$Tl (2614.5 keV). The symmetry assumptions and corrections described by McCay et al.[9] were adopted for the calibrations and trial surveys. All concentrations were recorded as relative values during acquisition in the test trials of the system.

### *Measurements and analyses*

The $^{40}$K nuclide emits a single gamma ray with an energy of 1460.8 keV and this decay alone was used to obtain the relative concentrations of natural potassium in an area. The nuclide $^{40}$K has an abundance of 0.0117% of the weight of naturally occurring potassium.[10] The $^{40}$K emission is commonly very strong in natural spectra, as a result of the abundance of potassium in nature. An active stabilisation function in the winTMCA32 software was used to correct for energy drift, which results from temperature changes while sites are surveyed. The 1460.8 keV emission of $^{40}$K was chosen as centroid for stabilisation and the fine gain was automatically adjusted by the winTMCA32 software to correct for any drift from the peak.

Thorium ($^{232}$Th) and uranium ($^{238}$U) concentrations are typically determined from the decay of daughter nuclides in the respective decay chains of these elements. Various cascades of gamma rays are emitted by the daughters of uranium and thorium, consequently resulting in several convoluted peaks in the recorded gamma ray spectra. This result is especially true when NaI(Tl) detectors, which have poor resolution power, are utilised for measurements. Thus several of the gamma ray cascades of the daughters of uranium and thorium are superimposed. However, because of the low cost and high effectiveness of NaI(Tl) scintillation detectors, they continue to be the preferred choice for in-situ measurements.

Five counting windows, or regions of interest (ROIs), positioned on the six gamma ray emissions were used to extract the thorium and uranium

concentrations. These ROIs were 238.6 keV ($^{212}$Pb), 351.9 keV ($^{214}$Pb), 583.2 keV ($^{208}$Tl), 609.3 keV ($^{214}$Bi), 1764.5 keV ($^{214}$Bi) and 2614.5 keV ($^{208}$Tl). The daughter nuclide from which the gamma ray emissions originates is indicated in brackets after each energy value. The proximity of the $^{208}$Tl (583.2 keV) and the $^{214}$Bi (609.3 keV) peaks resulted in a ROI with a combined count for $^{238}$U and $^{232}$Th. These combined counts in the convoluted peak, with the centroid at 596.0 keV, were also extracted. The combined counts in this ROI are useful as a result of the relationship that regularly exists between thorium and uranium concentrations in rock and soil.[11-13] All the ROIs that were used to extract the count rates of the naturally occurring nuclides are illustrated in Figure 2.

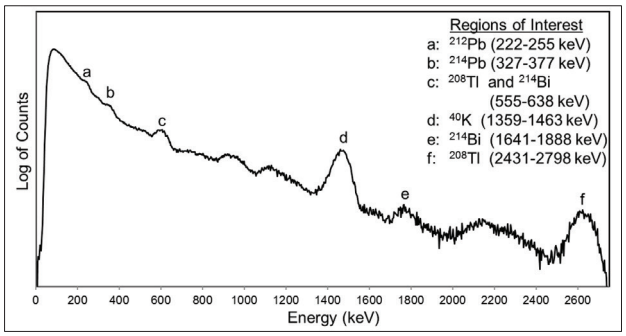


**Figure 2:** An in-situ gamma ray spectrum that indicates the six counting windows or regions of interest that were used to extract the relative concentrations of potassium, thorium and uranium.

The count rates in each ROI do not directly translate to the absolute concentrations for the various naturally occurring radionuclides. The counts do, however, provide a reasonable indication of the concentrations of the different radionuclides and the count rates were therefore inferred as concentrations. For the purposes of this article the concentrations will consequently be expressed as relative concentrations. These relative concentrations for potassium, uranium and thorium were subsequently classified and grouped with the help of GIS software. The potassium, uranium and thorium concentrations were then colour graded in red, blue and green, respectively. Darker shades of the colours indicate higher concentrations of the specific element. The graded colour symbols were then overlaid on Google Earth images, with the help of Quantum GIS software. These images are shown in Figures 3 to 8.

## Results and discussion

The measuring system was initially mounted on a quad motorcycle and tested in a nature reserve close to the town of Saldanha on the west coast of South Africa. This reserve was selected based on the availability of radiation data from previous studies[8,14] as well as the unique geological features of the area. The nature reserve is characterised by multiple granite outcrops and soils in the reserve are also mainly granite based, as there is little input of material from elsewhere. Thus the reserve provides a test area dominated by granite, which has high levels of natural radioactivity; granite-rich areas consequently provide interesting radiation characteristics.[15,16]

The route started in a light residential zone with tar roads and continued along a dirt track into the nature reserve. The relative potassium, uranium and thorium concentrations are plotted in Figures 3, 4 and 5, respectively. The highest levels of potassium were measured in an area that was previously investigated and this area is indicated by the dashed ovals on the figures. This previous study investigated anthropogenic disturbances that took place during World War II[8] and found high potassium concentrations in this area. The higher potassium concentrations of the test trials that are demonstrated in the dashed oval in Figure 3 therefore correlated with these previous findings.

The relative uranium concentrations in Figure 4 were extracted according to a method that was proposed by Bezuidenhout[7] in which the 351.9 keV ROI of the $^{214}$Pb daughter nuclide was utilised for analyses. A similar method was adapted for the extraction of thorium by employing the 238.6 keV ROI of the $^{212}$Pb daughter nuclide (Figure 5). The highest levels of uranium and thorium on this route were measured on newly constructed tar roads in the small settlement. This is clearly visible in the northern section of the tracks in Figures 4 and 5.

Comparing Figure 4 with Figure 5 it is clear that the variations of the relative uranium concentrations correspond well with that of thorium. This relation between the uranium and thorium concentrations is not unusual for areas dominated by igneous geology.[11,17] The relative uranium and thorium concentrations in the area where anthropogenic disturbances took place are also notably different from that on the rest of the trial in the reserve (see dashed ovals in Figures 4 and 5). These higher uranium and thorium concentrations of the test trials also correlated with the findings of similarly elevated levels in the previous study.[8]

The system was also tested on the east coast of South Africa, close to the town of Amanzimtoti. As vehicles are not allowed on the beach, the system was carried on foot while measurements were conducted.

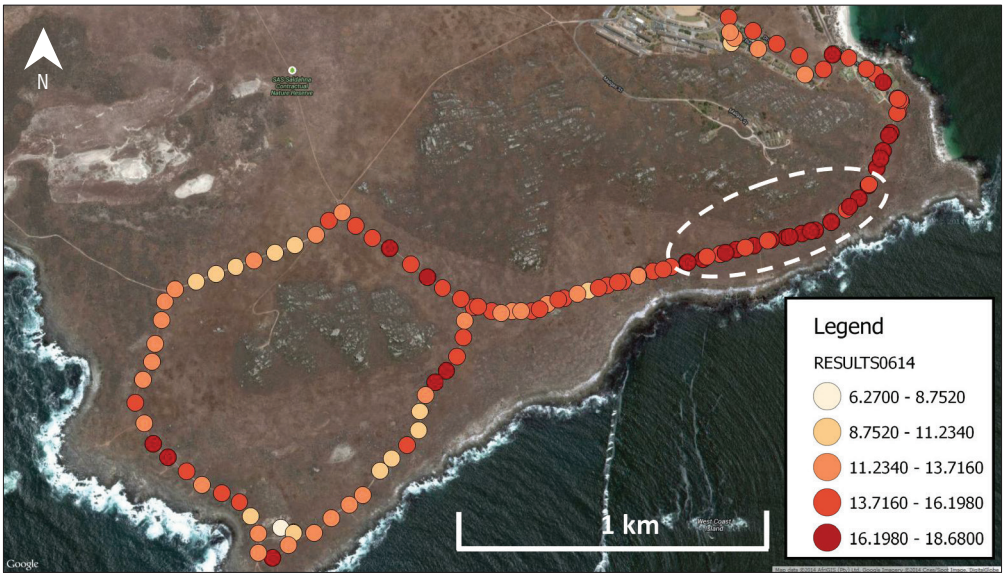


**Figure 3:** A Google Earth image indicating the relative potassium concentrations in the Saldanha Bay nature reserve, South Africa. The colour graded overlay displays the gamma ray counts in the region of interest around the 1460.8 keV gamma ray emission.


**Figure 4:** A Google Earth image indicating the relative uranium concentrations in the Saldanha Bay nature reserve, South Africa. The colour graded overlay displays the gamma ray counts in the region of interest around the 351.9 keV gamma ray emission.

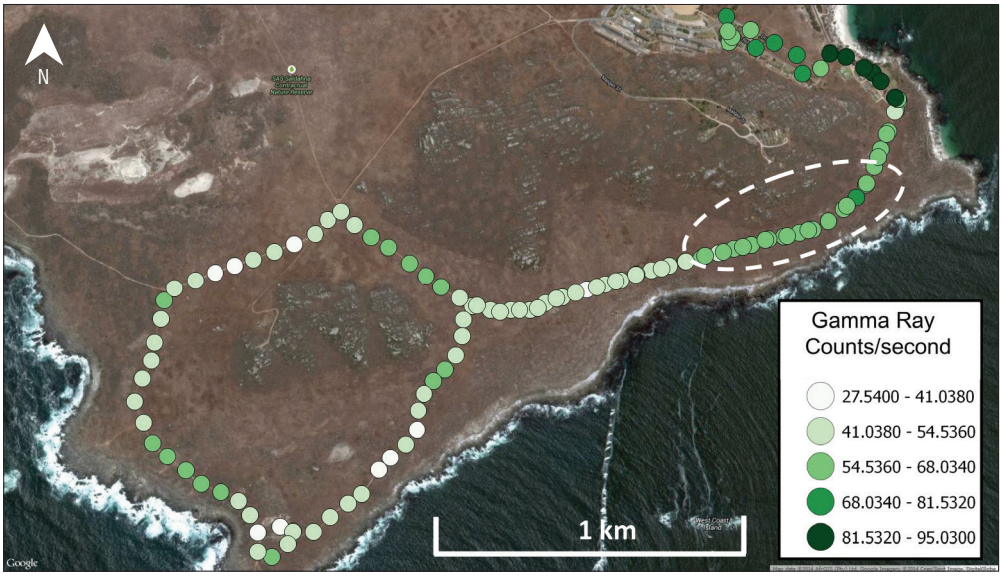


**Figure 5:** A Google Earth image indicating the relative thorium concentrations in the Saldanha Bay nature reserve, South Africa. The colour graded overlay displays the gamma ray counts in the region of interest around the 238.6 keV gamma ray emission.

The relative potassium concentration results are presented in Figure 6. Concentrations varied noticeably along the beach; the sections where elevated potassium concentrations were measured coincided with outlets of storm water pipes. Organic materials are usually relatively rich in potassium as a consequence of the prevalence of water-soluble potassium chloride in nature. Potassium-rich deposits therefore most likely settle in the parts of the beach where storm water runs off to the ocean.

The beach was also measured in a transect perpendicular to the shoreline in order to investigate the variation of nuclide concentrations with relations to the distance from the surf line (see the line indicated by a dashed oval on the image). These measurements indicated low levels of potassium concentrations in the section of the coastline furthest from the surf line. Dunes and sand in these furthest areas are usually mainly influenced by aeolian processes, whereas sand closest to the breaker line is mainly affected by littoral processes. The different processes may have different impacts on the potassium concentrations in the sand. The relation between potassium concentrations and the sand sedimentation processes requires further investigation.

The measuring system was lastly mounted in a motor vehicle and measurements were done at higher speeds on dirt and tar roads in the west coast region of South Africa. The results for the relative uranium and thorium concentrations for one such route are plotted on Google Earth images in Figures 7, 8 and 9.

Figure 7 and Figure 9 show the relative concentrations that were extracted from the traditional ROIs that are associated with uranium and thorium, namely 1764.5 keV and 2614.5 keV, respectively. The 351.9 keV ROI associated with uranium and the 238.6 keV ROI associated with thorium were also used to determine the relative concentrations. Figure 8 shows the relative uranium concentrations that were extracted from the 351.9 keV ROI and the results correlate well with the relative uranium

concentrations that were deduced from the traditional ROI (Figure 7). The relative concentrations that were extracted from the two ROIs that are associated with thorium also correlated well.

The higher count rates at the ROIs within the lower energy range of the spectra are mainly a result of detector efficiency characteristics. There are, however, gamma ray emissions from other daughters of the naturally occurring radionuclides that interfere with these ROIs. However, the good correlations between the various ROIs that were associated with uranium and thorium suggest that these interferences are negligible. The use of these non-traditional ROIs for analyses is mainly motivated by the substantially higher count rates compared with the count rates of the traditional ROIs. This finding supports the use of these non-traditional ROIs for in-situ analyses and measurements, which is of particular importance if dynamic surveys are conducted at higher speeds, resulting in shorter detector exposure times.

The highest levels of uranium and thorium were measured on recently constructed tar roads that carry high volumes of traffic. This observation is evident on the coloured overlay for straight roads on the western edges of the images in Figure 8 and Figure 9. Large but similar variations in uranium and thorium concentrations are also visible in the images. The variations of uranium concentrations correspond to that of thorium, for reasons similar to those discussed earlier in this section.

The lowest levels of uranium and thorium were measured on an old tar road and this road is indicated by dashed ovals on Figures 7, 8 and 9. It might be that the older roads were not constructed using the same techniques as those employed for the newer roads. For example, if less gravel was used in the construction, there would be a lower radiation signature. A further study is planned to investigate the correlation between the strength of tar roads and their radiation signatures.


**Figure 6:** A Google Earth image indicating the relative potassium concentrations on the north beach of Amanzimtoti, South Africa. The colour graded overlay displays the gamma ray counts in the region of interest around the 1460.8 keV gamma ray emission.


**Figure 7:** A Google Earth image indicating the relative uranium concentrations on tarred roads of the West Coast of South Africa. The colour graded overlay displays the gamma ray counts in the region of interest around the 1764.5 keV gamma ray emission.


**Figure 8:** A Google Earth image indicating the relative uranium concentrations on tarred roads of the West Coast of South Africa. The colour graded overlay displays the gamma ray counts in the region of interest around the 351.9 keV gamma ray emission.


**Figure 9:** A Google Earth image indicating the relative potassium concentrations on tarred roads of the West Coast of South Africa. The colour graded overlay displays the gamma ray counts in the region of interest around the 2614.5 keV gamma ray emission.

The measurements that we conducted at higher speeds from the motor vehicle gave good and consistent results, supporting the use of the system in such a manner and the use of the alternative ROIs for uranium and thorium concentration analyses.

## Conclusions

The necessity arose for a robust and highly transportable gamma ray field survey system that could be used in geographically remote areas in southern Africa. Various new technical advances provided the opportunity for the development of such a unique field measuring system. The required specifications for the measuring system were achieved by integrating a NaI(Tl) scintillation detector with a rugged Trimble tablet PC and an on-board GPS. The system is managed in real time by analyses software. The system acquires gamma ray spectra, extracts radionuclide concentrations and finally interpolates data to provide radionuclide concentrations and produce maps while on location.

The system was tested in different geographical settings and by different means of transport which included a motor vehicle, a quad motorcycle and by carrying the system on foot. Novel analyses methods were also developed in order to extract nuclide concentrations from the in-situ acquired spectra. The results from different geographical areas displayed variation in radiation well and also reproduced results from previous studies. There was also consistency across results that were obtained using the different analyses methods. These findings support the viability of various means of in-situ transport as well as the different in-situ analyses methods.

It is planned that this system, utilising multiple platforms of transport, will be used in several future studies in southern Africa. One potential study is to further map nuclide concentrations in coastal sediment[18] along the South African and Angolan coastlines in order to develop a model for coastal sediment transportation. Additionally, another investigation will look at the relationship between radiation signatures of tar roads and the

road quality. The development of this transportable radiation measuring system makes these and other studies both cost and time effective.

## Acknowledgements

I thank the National Research Fund of South Africa and Stellenbosch University for providing the funding for various aspects of this research.

## References

1. Tyler AN. High accuracy in situ radiometric mapping. J Environ Radioact. 2004;72:195–202. http://dx.doi.org/10.1016/S0265-931X(03)00202-9
2. Nilsson JMC, Östlund K, Söderberg J, Mattsson S, Rääf C. Tests of HPGe- and scintillation-based backpack γ-radiation survey systems. J Environ Radioact. 2014;135:54–62. http://dx.doi.org/10.1016/j.jenvrad.2014.03.013
3. Déjeant A, Bourva L, Sia R, Galoisy L, Calas G, Phrommavanh V, Descostes M. Field analyses of 238U and 226Ra in two uranium mill tailings piles from Niger using portable HPGe detector. J Environ Radioact. 2014;137105–112. http://dx.doi.org/10.1016/j.jenvrad.2014.06.012
4. Van der Graaf ER, Koomans RL, Limburg J, De Vries K. In situ radiometric mapping as a proxy of sediment contamination: Assessment of the underlying geochemical and -physical principles. App Rad Iso. 2007;65(5):619–633. http://dx.doi.org/10.1016/j.apradiso.2006.11.004
5. Hendriks PHGM, Limburg J, De Meijer RJ. Full-spectrum analysis of natural γ-ray spectra. J Environ Radioact. 2001;53:365–380. http://dx.doi.org/10.1016/S0265-931X(00)00142-9
6. Chiozzi P, De Felice P, Fazio A, Pasquale V, Verdoy M. Laboratory application of NaI(Tl) γ-ray spectrometry to studies of natural radioactivity in geophysics. App Rad Iso. 2000;53:127–132. http://dx.doi.org/10.1016/S0969-8043(00)00123-8
7. Bezuidenhout J. Measuring naturally occurring uranium in soil and minerals by analysing the 352 keV gamma-ray peak of 214Pb using a NaI(Tl)-detector. App Rad Iso. 2013;80:1–6. http://dx.doi.org/10.1016/j.apradiso.2013.05.008
8. Bezuidenhout J. Mapping of historical human activities in the Saldanha Bay military area by using in situ gamma ray measurements. Scientia Militaria. 2012;40(2):89–101.
9. McCay T, Harley TL, Younger PL, Sanderson DCW, Cresswell AJ. Gamma-ray spectrometry in geothermal exploration: State of the art techniques. Energies. 2014;7(8):4757–4780. http://dx.doi.org/10.3390/en7084757
10. National Institute of Standards and Technology, Physical Measurement Laboratory. Atomic weights and isotopic compositions with relative atomic masses [database on the Internet]. No date [cited 2015 Aug 24]. Available from: http://www.nist.gov/pml/data/comp.cfm
11. Montes ML, Mercader RC, Taylor MA, Runco J, Desimoni J. Assessment of natural radioactivity levels and their relationship with soil characteristics in undisturbed soils of the northeast of Buenos Aires province, Argentina. J Environ Radioact. 2012;105:30–39. http://dx.doi.org/10.1016/j.jenvrad.2011.09.014
12. Abbady AGE, El-Arabi AM, Abbady A. Heat production rate from radioactive elements in igneous and metamorphic rocks in Eastern Desert, Egypt. App Rad Iso. 2006;64:131–137. http://dx.doi.org/10.1016/j.apradiso.2005.05.054
13. Abbady AGE. Evaluation of heat generation by radioactive decay of sedimentary rocks in Eastern Desert and Nile Valley, Egypt. App Rad Iso. 2010;68:2020–2024. http://dx.doi.org/10.1016/j.apradiso.2010.03.023
14. Bezuidenhout J. Using GIS to estimate background radiation levels. PositionIT Magazine. 2013 April/May;65–73.
15. Llope WJ. Activity concentrations and dose rates from decorative granite countertops. J Environ Radioact. 2011;102:620–629. http://dx.doi.org/10.1016/j.jenvrad.2011.03.012
16. Baranwal VC, Sharma SP, Sengupta D, Sandilya MK, Bhaumik BK, Guin R, et al. A new high background radiation area in the geothermal region of Eastern Ghats Mobile Belt (EGMB) of Orissa, India. Rad Meas. 2006;41:602–610. http://dx.doi.org/10.1016/j.radmeas.2006.03.002
17. Abbady AGE, El-Arabi AM, Abbady A. Heat production rate from radioactive elements in igneous and metamorphic rocks in Eastern Desert, Egypt. App Rad Iso. 2006;64:131–137. http://dx.doi.org/10.1016/j.apradiso.2005.05.054
18. Thereska J. Natural radioactivity of coastal sediments as tracer in dynamic sedimentology. Nukleonika. 2009;54(1):45–50.